

**Original citation:**

Liu, Teng, Gao, Weiguo, Tian, Yanling, Zhang, Dawei, Zhang, Yifan and Chang, Wenfen. (2017) Power matching based dissipation strategy onto spindle heat generations. Applied Thermal Engineering, 113. pp. 499-507.

**Permanent WRAP URL:**

<http://wrap.warwick.ac.uk/94048>

**Copyright and reuse:**

The Warwick Research Archive Portal (WRAP) makes this work by researchers of the University of Warwick available open access under the following conditions. Copyright © and all moral rights to the version of the paper presented here belong to the individual author(s) and/or other copyright owners. To the extent reasonable and practicable the material made available in WRAP has been checked for eligibility before being made available.

Copies of full items can be used for personal research or study, educational, or not-for-profit purposes without prior permission or charge. Provided that the authors, title and full bibliographic details are credited, a hyperlink and/or URL is given for the original metadata page and the content is not changed in any way.

**Publisher's statement:**

© 2017, Elsevier. Licensed under the Creative Commons Attribution-NonCommercial-NoDerivatives 4.0 International <http://creativecommons.org/licenses/by-nc-nd/4.0/>

**A note on versions:**

The version presented here may differ from the published version or, version of record, if you wish to cite this item you are advised to consult the publisher's version. Please see the 'permanent WRAP URL' above for details on accessing the published version and note that access may require a subscription.

For more information, please contact the WRAP Team at: [wrap@warwick.ac.uk](mailto:wrap@warwick.ac.uk)

# 1 Power Matching Based Dissipation Strategy onto 2 Spindle Heat Generations

3 Teng Liu<sup>1,2</sup>, Weiguo Gao<sup>1\*</sup>, Yanling Tian<sup>1,5</sup>, Dawei Zhang<sup>1</sup>, Yifan Zhang<sup>3</sup>, and Wenfen Chang<sup>1,4</sup>

4 <sup>1</sup> *Key Laboratory of Mechanism Theory and Equipment Design of Ministry of Education, Tianjin*  
5 *University, Tianjin 300354, China*

6 <sup>2</sup> *School of Mechanical Engineering, Hebei University of Technology, Tianjin 300130, China*

7 <sup>3</sup> *School of Electrical Engineering and Automation, Tianjin University, Tianjin 300072, China*

8 <sup>4</sup> *Beijing Precision Machinery & Engineering Research Co., Ltd., Beijing 101312, China*

9 <sup>5</sup> *School of Engineering, University of Warwick, Coventry, CV4 7AL, UK*

10

11 **Abstract:** To overcome the imbalance between spindle heat generation and dissipation caused  
12 by existed spindle cooling strategies, this paper develops a power matching based cooling  
13 strategy for motorized spindle unit. Firstly, heat generation, conduction and dissipation are  
14 considered for the modeling of spindle structural heat exchange. This modeling methodology  
15 conveys that an operating motorized spindle unit will have satisfactory thermal behaviors only  
16 if the supply dissipation powers from recirculation coolants are dynamically and respectively  
17 equal to their corresponding heat generation powers (mainly from spindle bearings and motor).  
18 Based on this principle, the power matching between spindle heat generations and dissipations  
19 is realized by the real-time power estimations of spindle heat sources and the modified constant  
20 supply cooling powers strategy. It can be ultimately verified by experiments that the power  
21 matching based dissipation strategy is more advantageous than existed spindle cooling  
22 strategies in dissipation of spindle heat generations and decrease of thermal errors.

23 **Keywords:** Power matching, Dissipation strategy, Motorized spindle unit, Heat generation,  
24 Thermal error

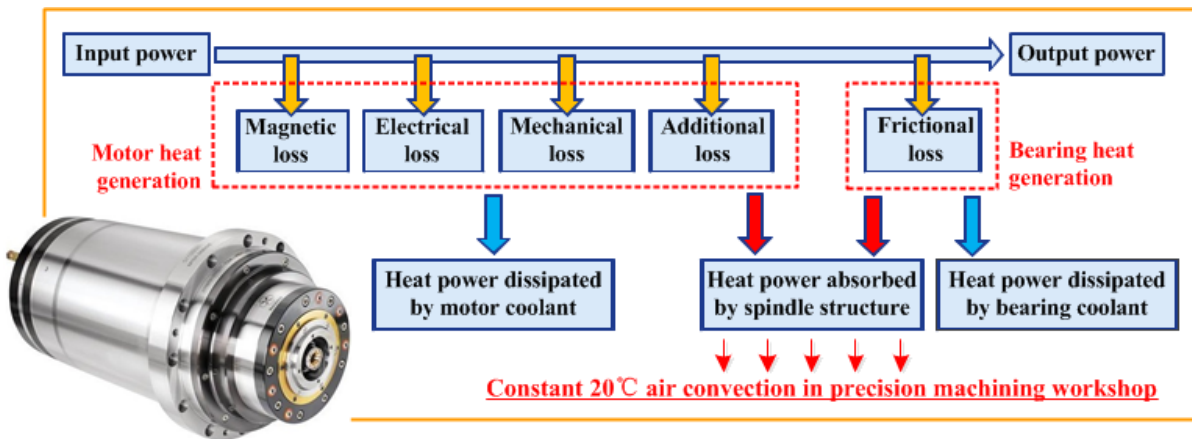
25

26 \*E-mail address of the corresponding author: gaowg@tju.edu.cn

27

1 **1 Introduction**

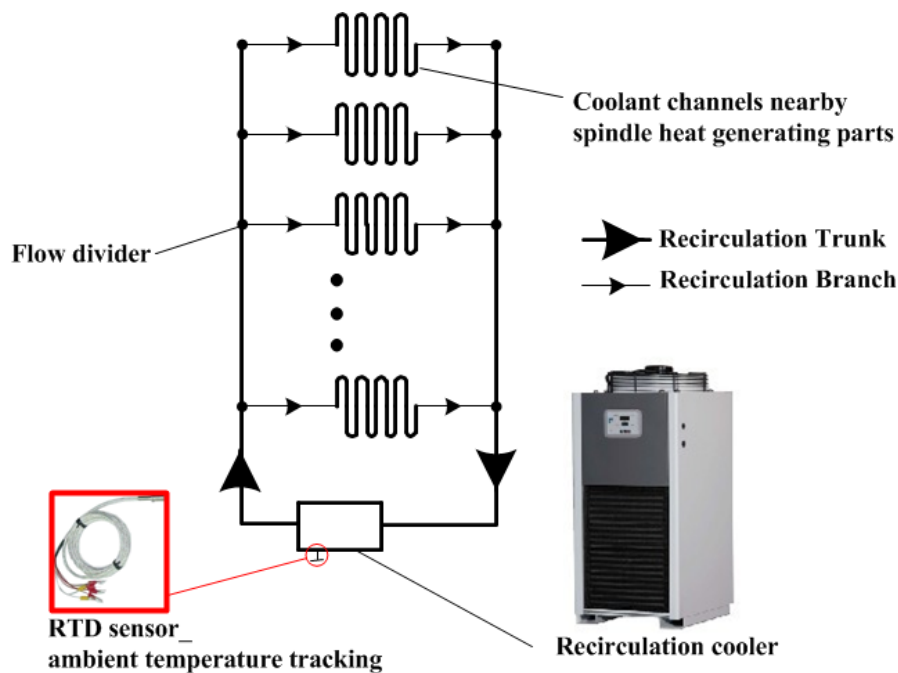
2 Motorized spindle unit, being the **crucial** component of precision machine tools, can realize  
3 various machining types such as drilling, milling, grinding and so on. Generally, the motorized  
4 spindle unit has a compact structure **combining** its built-in motor and high speed bearings. This  
5 structure provides motorized spindle unit with not only high speed, precision, and rigidity, but  
6 also some thermal disturbances **on** precision machining accuracy and accuracy stability <sup>[1]</sup>. As  
7 illustrated in Fig. 1, there are mainly the motor and bearing power **losses** in the energy  
8 conversion of a motorized spindle unit operating in a constant temperature (20°C) workshop for  
9 precision machining <sup>[2]</sup>. The former includes motor magnet loss, electric loss, mechanical loss  
10 and some additional **losses**, and the latter is mainly attributed to the friction between bearing  
11 parts. Generally, the overwhelming majorities of these power losses contribute to the spindle  
12 internal heat generations, to cause the spindle thermal deformation errors for machining  
13 accuracy degradation. **To solve** this problem, recirculation coolants are always applied onto the  
14 spindle motor and bearings to realize dissipation management onto their heat generations  
15 caused by power **losses**, **and to** reduce the harmful heat absorbed by spindle structure <sup>[3, 4]</sup>.



16  
17 Fig. 1 Energy conversion of an operating motorized spindle unit

18 However, although recirculation coolants can improve the thermal behaviors of motorized  
19 spindle unit, the deficiencies of its traditional uniform and open-loop strategy are being exposed  
20 with the rapid evolution of precision machining. As revealed in Fig. 2: On one hand, the  
21 traditional strategy for spindle recirculation cooling is based on flow divider to realize parallel  
22 coolants from one recirculation cooler, which means different spindle heat generating parts **with**

1 various heat generation scales are forced to bear an uniform supply cooling temperature. This  
 2 can generally result in the heat exchange imbalance of spindle structure. On the other hand, the  
 3 traditional strategy always has the open-loop temperature control method. Its supply cooling  
 4 temperature is generally determined based on the preset constant instruction or the ambient  
 5 temperature tracked by Resistive Thermal Detector (RTD) sensors, and thus it is hardly to be  
 6 adjusted dynamically according to the spindle time-varying thermal behaviors in operation.  
 7 This can give rise to the incompleteness and instability of the spindle structural heat dissipation.  
 8 All these insufficiencies can weaken the effectiveness of traditional cooling strategy for  
 9 reducing the spindle thermal errors [5, 6].



11 Fig. 2 Principle of traditional strategy for spindle recirculation cooling

12 To overcome these disadvantages of traditional uniform and open-loop cooling strategy, a  
 13 differentiated multi-loops bath recirculation system was developed in our previous study [7]. On  
 14 this basis, being the preliminary attempt to differentiated and closed-loop dissipation strategy  
 15 for spindle internal heat generations, the constant supply cooling powers strategy was proposed.  
 16 This strategy was experimentally verified to be more efficient in improving the spindle thermal  
 17 behaviors than traditional strategy. However, from the perspective of spindle energy exchange,  
 18 this strategy can reach the time-averaged spindle cooling effect exclusively, but hardly realize

1 the real-time and accurate dissipations onto the spindle time-variant heat generations, which are  
2 closely related to spindle working conditions.

3 For the realization of the real-time power matching between spindle heat generations and  
4 dissipations, this paper makes modifications based on constant supply cooling powers strategy,  
5 to construct a power matching based dissipation strategy for internal heat generations of  
6 motorized spindle unit. This strategy can realize the sufficient dissipations of spindle internal  
7 heat generations, for further improvements of spindle accuracy and accuracy stability. The  
8 remainder of the paper is organized as follows: Section 2 establishes the models of the  
9 theoretical interaction among structural heat generations, dissipations and conductions of the  
10 operating motorized spindle unit, and then obtains the relationships with other spindle thermal  
11 behaviors. Based on these analyses, Section 3 proposes the realization method of the power  
12 matching based dissipation strategy for spindle heat generations. Section 4 analyzes the  
13 methods and results of the advantageous verification experiments for the developed power  
14 matching based spindle cooling strategy. Section 5 gives the conclusions of the whole study.

## 15 **2 Theoretical model for power matching based dissipation strategy for spindle internal** 16 **heat generations**

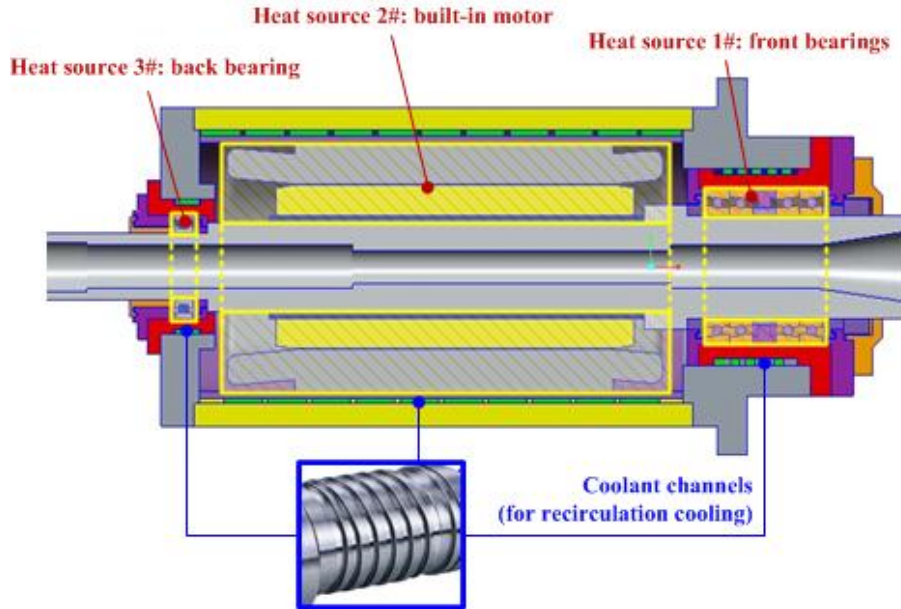
17 In this section, the general interaction of the internal heat generation, dissipation and  
18 conduction of an operating motorized spindle unit is analyzed, and then the theoretical  
19 association with spindle thermal deformation behaviors is investigated, finally the theoretical  
20 guidance for the power matching based dissipation strategy for spindle internal heat generation  
21 is formed.

### 22 **2.1 Spindle structural heat exchange - thermal deformation modeling**

23 The physical structure of a typical type of motorized spindle unit is illustrated in Fig. 3: Its  
24 main heat sources (heat generating parts) are front bearings, back bearing and built-in motor of  
25 the spindle. Meanwhile, 3 coolant channels are designed around these heat sources respectively  
26 to realize recirculation cooling effects for dissipations of their heat generations. When the  
27 motorized spindle unit is operating in a constant 20°C workshop, its heat conductions  $\Phi_{\text{con}}$  (W)  
28 are closely associated with its heat generations  $\Phi_{\text{gen}}$  (W) and dissipations  $\Phi_{\text{coo}}$  (W), which is

1 described in Fig. 4. Then according to energy conservation law, the spindle temperature  
 2 distribution can be calculated as [8]:

$$3 \quad \sum \Phi = \Phi_{\text{gen}} - \Phi_{\text{coo}} + \Phi_{\text{con}} = c_T \frac{dT}{d\tau} \quad (1)$$



4  
 5 Fig. 3 Design of spindle heat sources and coolant channels

6 In equation (1),  $c_T$  is heat capacitance (J/°C), and the heat conduction ( $\Phi_{\text{con}}$ ) through a cross  
 7 section of spindle continuous material is [9]:

$$8 \quad \Phi_{\text{con}} = \lambda S \frac{dT}{dx} \quad (2)$$

9 In equation (2),  $S$  is the area perpendicular to the direction of heat flux (m<sup>2</sup>);  $\lambda$  is the thermal  
 10 conductivity (W/(m•°C)).

11 Being the source for spindle thermal errors, thermal deformation of the spindle structure is  
 12 analyzed based on the thermal deformation  $\Delta L$  of one dimensional rod with constraints:

1

$$\begin{cases} \Delta L = \alpha L(T_i - T_{i-1}) + \frac{\sigma L}{E} \\ \Delta L = \frac{-P}{j} \\ P = A\sigma \end{cases} \quad (3)$$

2

3

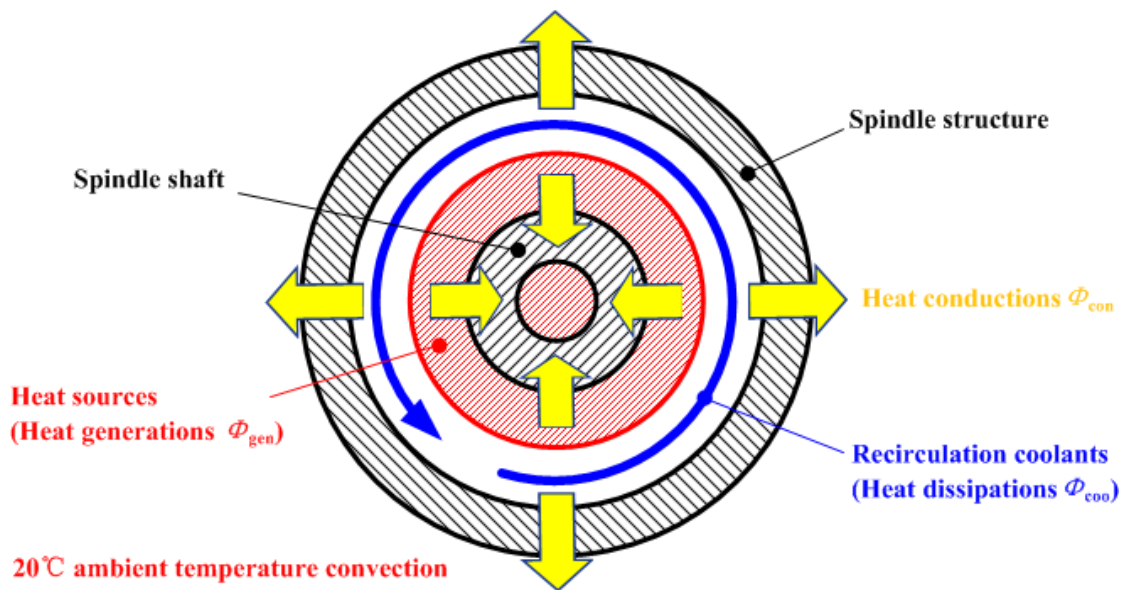
4

5

In equation (3),  $L$  is the original length (m);  $T_i$  and  $T_{i-1}$  are the temperatures at  $\tau_i$  moment and  $\tau_{i-1}$  moment ( $^{\circ}\text{C}$ );  $\alpha$  is the thermal expansion coefficient ( $^{\circ}\text{C}^{-1}$ );  $\sigma$ ,  $P$ ,  $E$ ,  $j$  and  $A$  are the stress (MPa), the axial force (N), the modulus of elasticity ( $\text{N}/\text{m}^2$ ), the axial stiffness ( $\text{N}/\text{m}$ ) and the area of the cross section ( $\text{m}^2$ ) respectively. Then equation (3) can be simplified as:

6

$$\Delta L = \frac{\alpha L(T_i - T_{i-1})}{1 + \frac{jL}{AE}} \quad (4)$$



7

8

Fig. 4 Association of spindle heat generations, dissipations and conduction

9

## 2.2 Heat power measures for constantly least thermal deformation of spindle structure

10

11

For the **improvement** of precision machining accuracy and accuracy stability, the least thermal errors of operating motorized spindle unit can be realized consistently by the avoidance

1 of spindle structural thermal deformation. According to equation (4), the thermal deformation of  
2 spindle structure can be theoretically equal to zero only if the spindle temperature meets:

$$3 \quad T_i - T_{i-1} \cong \frac{dT}{d\tau} = 0 \quad (5)$$

4 It is assumed that motorized spindle unit has the structure-averaged temperature distribution  
5 (=20°C ambient temperature) at the initial state of spindle operation, which means:

$$6 \quad \frac{dT}{dx} = 0 \quad (6)$$

7 Equations (5) - (6) can be substituted into Equations (1) - (2) to obtain heat power measures  
8 for persistent realization of structure-averaged spindle temperature distribution, at any operating  
9 moment  $\tau$ :

$$10 \quad \Phi_{\text{gen}} = \Phi_{\text{coo}} \quad (7)$$

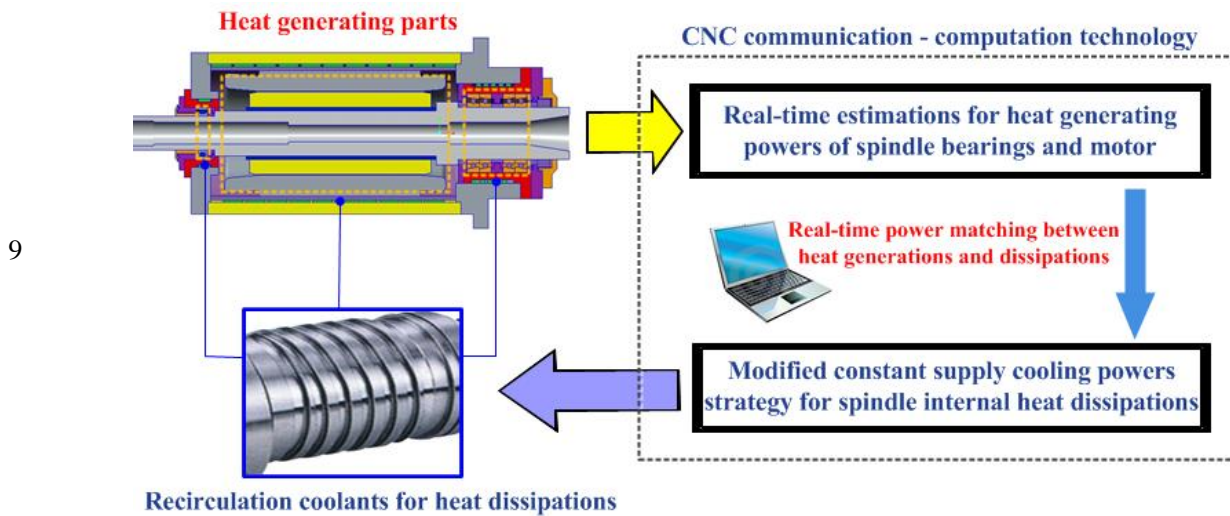
11 Equation (7) clarifies the core principle of the power matching based dissipation strategy for  
12 internal heat generations of operating motorized spindle unit, which will be developed and  
13 introduced in Section 3. Generally, the spindle internal heat generations  $\Phi_{\text{gen}}$  in equation (7)  
14 have time-variant scales, because they are directly affected by the spindle working conditions  
15 including rotation speed and cutting loads. Therefore, the realization of real-time power  
16 matching between spindle heat generations and dissipations must be based on the differentiated  
17 and closed-loop cooling strategy for the motorized spindle unit in operation.

### 18 **3 Realization method of power matching based dissipation strategy for spindle internal** 19 **heat generations**

20 From precision machining perspectives, spindle thermal deformation errors are expected to  
21 be persistently eliminated for the satisfactory accuracy and accuracy stability, during precision  
22 machining activities. According to the conclusion in Section 2 that the least spindle thermal  
23 errors can be realized by the method of real-time and accurate dissipations of the spindle  
24 internal heat generations, the power matching based dissipation strategy for spindle internal  
25 heat generations has been developed, and its realization method is depicted in Fig. 5: On one



1 hand, the real-time heat power estimations of spindle bearings and motor are performed during  
 2 spindle operation. On the other hand, to **guarantee** the real-time power matching between  
 3 spindle heat generations and dissipations, the estimated heat power values are adopted for the  
 4 real-time calculations about the required supply cooling powers of recirculation coolants,  
 5 according to equation (7). The power matching between spindle heat generations and  
 6 dissipations is mainly realized based on CNC communication - computation technology, and  
 7 the calculated dissipation power values are **implemented** by the modified constant supply  
 8 cooling powers strategy <sup>[7]</sup> for the motorized spindle unit.



10 Fig. 5 Realization method of power matching based dissipation strategy onto spindle internal  
 11 heat generations

### 12 3.1 Real-time power estimations of spindle internal heat generations

#### 13 3.1.1 Power modeling of spindle internal heat generations

14 Heat power models of spindle bearings and motor are vital for real-time power estimation of  
 15 spindle internal heat generations, which is required by the **implementation** of power matching  
 16 based dissipation strategy. The heat power models of bearings and motor are established based  
 17 on their published methods respectively.

18 (i) Spindle bearings

1 Generally, the spindle bearing heat is generated in bearing contact areas due to the frictions  
 2 between balls and inner and outer races <sup>[10, 11]</sup>. Then the heat power  $\Phi_b$  (W) modeling of both  
 3 spindle front bearings and back bearing (in Fig. 3) can be determined by the following method:

$$4 \quad \Phi_b = 1.047 \times 10^{-4} n(M_0 + M_1) \quad (8)$$

5 In equation (8),  $n$  (r/min) is spindle rotating velocity, friction torque  $M_0$  (Nmm) brought by  
 6 bearing lubricant viscosity and friction torque  $M_1$  (Nmm) caused by bearing applied force can  
 7 be calculated respectively as:

$$8 \quad M_0 = \begin{cases} 10^{-7} f_0 (v_0 n)^{2/3} D_m^3, v_0 n \geq 2000 \\ 160 \times 10^{-7} f_0 D_m^3, v_0 n < 2000 \end{cases} \quad (9)$$

$$9 \quad M_1 = f_1 F_\beta D_m \quad (10)$$

10 In equations (9)-(10),  $f_0, f_1$  are parameters related to the type, structure, force and lubrication  
 11 of bearings;  $F_\beta$  (N) is the load determined by the magnitude and direction of the force onto  
 12 bearings;  $v_0$  (cSt) is the kinematic viscosity of lubricant;  $D_m$  (m) is the diameter of pitch circle.

13 It can be concluded by the modeling method that, heat powers of spindle bearings are directly  
 14 affected by spindle rotation speed and bearing loads, which is time-variant during the spindle  
 15 operation. Meanwhile, the bearing preload, type, structure, size and lubrication, which are  
 16 known and regarded as unchanged, also impact the scale of bearing heat generations.

17 (ii) Spindle motor

18 Heat generation power  $\Phi_m$  (W) of spindle motor is mainly attributed to its magnet loss  
 19  $P_h$  (W), electric loss  $P_{CU}$  (W) and mechanical loss  $P_f$  (W), with additional loss being ignored:

$$20 \quad \Phi_m = P_h + P_{CU} + P_f \quad (11)$$

21 For equation (11), the magnet loss  $P_h$  (W) contains hysteresis loss  $P_t$  (W) and eddy current  
 22 loss  $P$  (W), and they can be calculated by:

$$\begin{cases} P_t = C f B_{\max}^2 \\ P = \frac{\pi^2 t^2 (f B_{\max})^2}{6 \rho \gamma_c} \end{cases} \quad (12)$$

In equation (12),  $C$  is a constant value related to electrical steel grades;  $f$  ( $s^{-1}$ ) is magnetizing frequency;  $B_{\max}$  (T) is the maximum magnetic flux density;  $t$  (m) is the thickness of silicon steel sheet;  $\gamma_c$  ( $kg/m^3$ ) and  $\rho$  ( $\Omega m$ ) are the density and electrical resistivity of iron core respectively.

Besides, the electric loss  $P_{Cu}$  (W) in equation (11) can be calculated by:

$$P_{Cu} = \frac{I^2 \rho_c L}{S} \quad (13)$$

In equation (13),  $I$  (A) is the current;  $\rho_c$  ( $\Omega m$ ),  $L$  (m) and  $S$  ( $m^2$ ) are the resistivity, length, sectional area of a conductor.

Finally, the calculation method of mechanical loss  $P_f$  (W) in equation (11) is:

$$P_f = \pi C' \rho_{air} \omega^3 R_f^4 L_f \quad (14)$$

In equation (14),  $C'$  is the frictional coefficient;  $R_f$  (m) and  $L_f$  (m) are outer radius and length of rotor;  $\omega$  (rad/s) is the angular velocity of rotor;  $\rho_{air}$  ( $kg/m^3$ ) is the density of air.

During the spindle operation, time-variant factors influencing the motor heat generation scale mainly include spindle rotation speed and electricity. Besides, there are still some time-invariant factors, such as motor physical properties and structural scales, contributing to heat generation modeling of spindle motor.

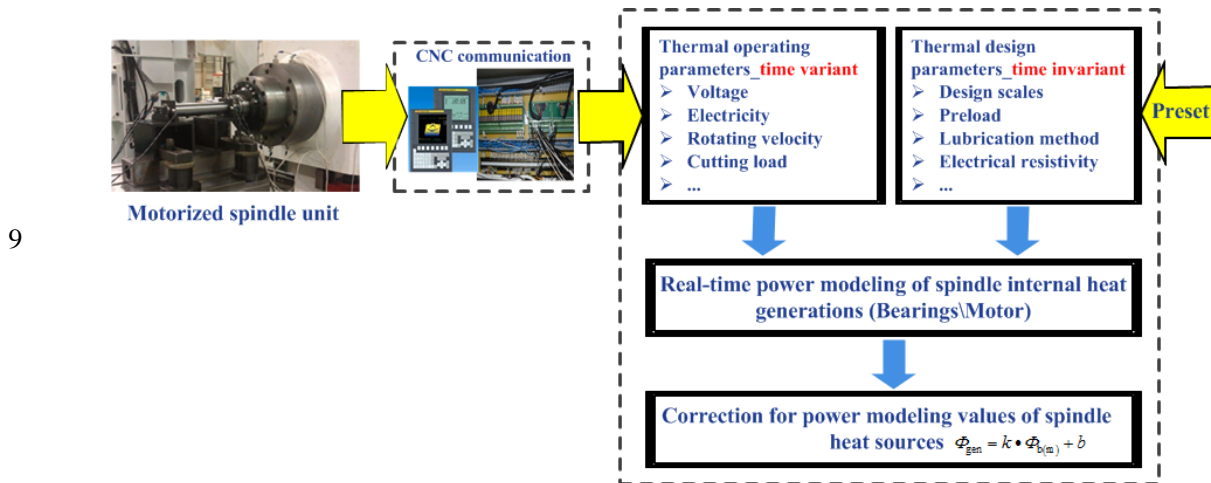
### 3.1.2 Realization of real-time power estimations of spindle internal heat generations

It can be concluded from Section 3.1.1 that, the power modeling of spindle heat sources must be done based on required parameters. Some of them are time-variant during the spindle operation, and the others are not. As shown in Fig. 6, the former must be monitored by CNC communication technology, and the latter can be preset in the host computer software, for the

1 realization of real-time power modeling of spindle internal heat generations. Generally, the  
 2 power modeling values of spindle heat sources have obvious inconsistencies with real ones.  
 3 Therefore, power modeling values of spindle heat sources must be corrected to finish their  
 4 real-time power estimations. The correction method is given as follows:

$$\Phi_{gen} = k \cdot \Phi_{b(m)} + b \quad (15)$$

6 In equation (15),  $k$  and  $b$  are the proportionality and deviation coefficient respectively for the  
 7 power modeling corrections of spindle heat sources. The determinations of them must be based  
 8 on the experimental trial and error method introduced in Section 3.2.3.



10 Fig. 6 Realization method of real-time power estimations of spindle internal heat generations

### 11 3.2 Real-time power determinations of spindle internal heat dissipations

#### 12 3.2.1 Power matching based modification onto constant supply cooling powers strategy

13 It can be observed from Fig. 3 that, in order to realize the dissipations of internal heat  
 14 generations of operating motorized spindle unit, coolant channels are designed for recirculation  
 15 coolants being applied nearby spindle heat sources (front bearings, motor and back bearing).  
 16 Meanwhile, these heat dissipations can bring the real-time coolant temperature rises between  
 17 outlets and inlets of coolant channels. Then these temperature rises can reflect the real-time  
 18 power scales  $\Phi_{coo}$  (W) of the spindle heat dissipations onto heat sources 1#–3# respectively by  
 19 the following method:

$$\Phi_{\text{cool}_i} = c\rho Q^i \Delta T_{\tau}^i, \quad i=1, 2, 3 \quad (16)$$

In equation (16),  $c$  (J/(kg·K)),  $\rho$  (kg/m<sup>3</sup>) and  $Q$  (L/min) are special heat, density and supply flow rate of recirculation coolants respectively;  $\Delta T_{\tau}$  (°C) is real-time coolant temperature rise between outlet and inlet of coolant channel. To be more advantageous than traditional cooling strategy for motorized spindle unit, the constant supply cooling powers strategy [7] was presented in our previous work. This strategy can realize constantly the expected dissipation powers of spindle recirculation coolants. Its principle is based on the differentiated realizations of objective scales of  $\Delta T_{\tau}$  for different spindle heat sources, with  $c$ ,  $\rho$  and  $Q$  being consistent with time.

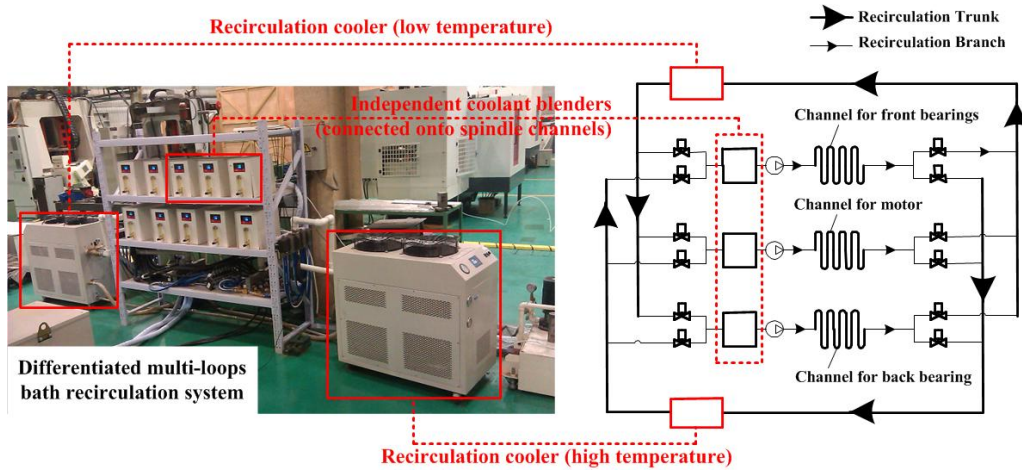
In this paper, constant supply cooling powers strategy is modified to be associated with the real-time power estimations of spindle internal heat generations, to realize the power matching between spindle heat generations and dissipations. Because of the time-variant property of spindle internal heat generations, real-time calculations of objective dissipation power scales onto spindle heat sources 1#–3# must be based on the equations (7), (15) and (16). Then the real-time calculation strategy for coolant supply temperatures  $T_{\text{su}}$  (°C) is constructed:

$$\begin{cases} \overline{\Delta T_{\tau}}^i = \frac{k_i \bullet \Phi_i + b_i}{c\rho Q^i}, i=1,2,3 \\ T_{\text{su}_r+1}^i = T_{\text{ou}_r}^i - \overline{\Delta T_{\tau}}^i \end{cases} \quad (17)$$

In equation (17),  $T_{\text{su}}$  (°C) and  $T_{\text{ou}}$  (°C) are the supply (inlet) and outlet temperature for spindle recirculation coolant respectively;  $\overline{\Delta T}$  (°C) is the objective coolant temperature rise between outlet and inlet of the coolant channel.

### 3.2.2 Realization of modified constant supply cooling powers strategy

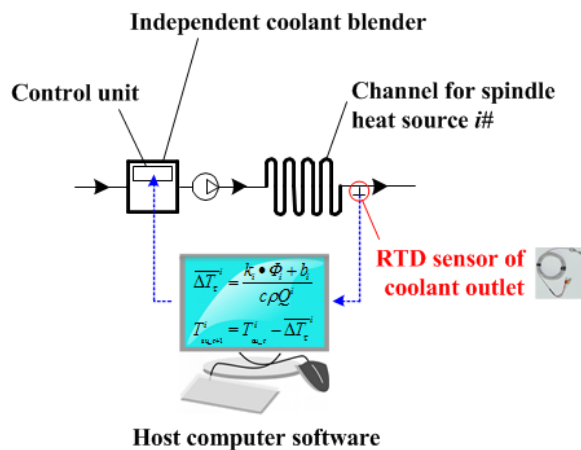
The presented spindle constant supply cooling powers strategy must be realized based on the previous differentiated multi-loops bath recirculation system. As revealed in Fig.7, 3 coolant channels of motorized spindle unit are equipped with 3 recirculation branches respectively of this system for different coolant supply temperatures onto spindle heat sources.



1

2 Fig. 7 Spindle coolant channels equipped with differentiated multi-loops bath recirculation  
3 system

4 Meanwhile, Fig. 8 expresses the realization principle of the constant supply cooling power in  
5  $i$ th recirculation branch ( $i=1, 2, 3$ ): The RTD sensor for coolant outlet temperature detection is  
6 used to trigger the real-time calculation in host computer software for the generation of supply  
7 temperature instructions. Specially, this calculation must be based on equation (17) with  $k$ ,  $b$ ,  
8  $c$ ,  $\rho$  and  $Q$  being consistent with time. The aim is to ensure the real-time power matching  
9 between spindle internal heat generations and dissipations.



10

11 Fig. 8 Realization method of modified constant supply cooling powers strategy in  $i$ th  
12 recirculation branch ( $i=1, 2, 3$ )

13 **3.2.3 Coefficient determinations for power matching based dissipation strategy for spindle**  
14 **heat generations**

1 In equation (17), the correcting coefficients  $k$  and  $b$  must be determined by the experimental  
2 trial and error method. It can be concluded from Section 2 that  $\Phi_{\text{gen}} = \Phi_{\text{coo}}$  is the very method  
3 realizing  $\frac{dT}{d\tau} = 0$  for an operating motorized spindle unit. Therefore, the determinations of  
4 coefficients  $k$  and  $b$  can be **conducted** by the trial and error method based on a series of spindle  
5 experiments. For **each** experiment, the motorized spindle unit is equipped with the power  
6 matching based dissipation strategy with random  $k$  and  $b$  values, and forced to have a regular  
7 3000 RPM rotation speed for 5 hours. The aim of these experiments is to find out the  
8 approximately appropriate values of correcting coefficients  $k$  and  $b$ , which can make the power  
9 matching based dissipation strategy ensure persistently  $\frac{dT}{d\tau} = 0$  during a spindle operation.

## 10 **4 Verification experiments**

11 For the power matching based dissipation strategy onto the spindle internal heat generations,  
12 its advantage in spindle structural heat dissipations is verified by experiments in this section.  
13 These experiments are performed with power matching based dissipation strategy and 2 **existed**  
14 spindle cooling strategies respectively.

### 15 **4.1 Experimental setup**

16 Beside the outlet temperature detections of spindle internal recirculation coolants above,  
17 there are some other thermal measurements about motorized spindle unit being adopted. As  
18 shown in Fig. 9, the structural temperature and thermal errors of motorized spindle unit were  
19 measured by the similar method of our previous study: On one hand, RTD sensors are located  
20 nearby spindle heat sources:  $T_A$  and  $T_B$  are measured **for** the temperature of front bearings;  
21  $T_C$ - $T_F$  stand for the motor temperature;  $T_G$  and  $T_H$  are used for detecting the back bearing  
22 temperature. On the other hand, the spindle thermal errors are detected by the eddy current  
23 displacement sensors based on inspection bar, and these sensors must be located according to  
24 standard method for the detection of spindle thermal errors<sup>[12]</sup>.



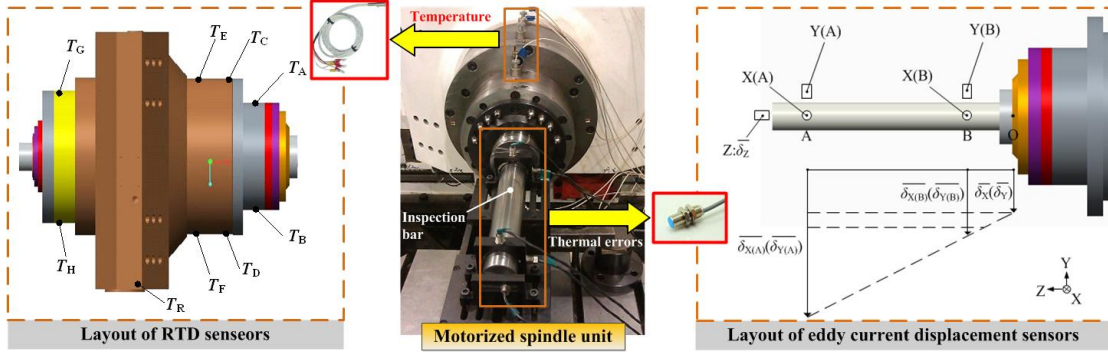


Fig. 9 Sensor layout for evaluations about spindle thermal behaviors

During experimental operations of motorized spindle unit, the detected outlet temperatures and real-time supply temperatures (inlet temperatures) of spindle coolants are monitored for the calculation of spindle dissipation powers onto heat sources 1#-3# respectively by equation (16). Meanwhile, the spindle structural temperatures and thermal errors are detected to evaluate the spindle thermal behaviors.

## 4.2 Experimental method

In order to verify the advantages of the presented power matching based dissipation strategy for spindle internal heat generations, the motorized spindle unit is operating under 3 different cooling strategies respectively: the traditional strategy (coolant supply temperatures are uniform and always equivalent to ambient temperature), the constant supply cooling powers strategy and the power matching based dissipation strategy.

For all the verification experiments: ① motorized spindle unit is operating from 1000RPM to 5000RPM (increasing step is 1000RPM), and every speed condition lasts for 1 hour; ② the experimental workshop has a constant temperature ( $T_{am}=20\pm0.3^{\circ}\text{C}$ ); ③ the density  $\rho$ , special heat  $c$  and supply flow rate  $Q$  of adopted recirculation coolants are  $910\text{ kg/m}^3$ ,  $2090\text{ J/(kg}\cdot\text{K)}$  and  $5\text{L/min}$ , respectively.

## 4.3 Experimental results and discussions

### 4.3.1 Spindle internal heat generations and dissipations

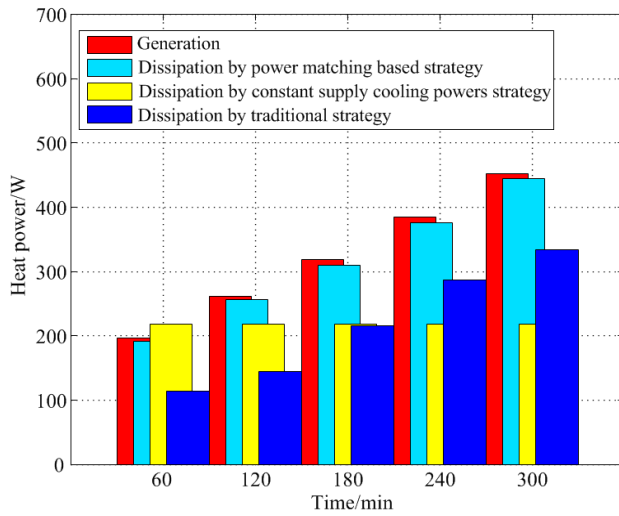
In order to verify the advantage of the power matching based dissipation strategy in spindle



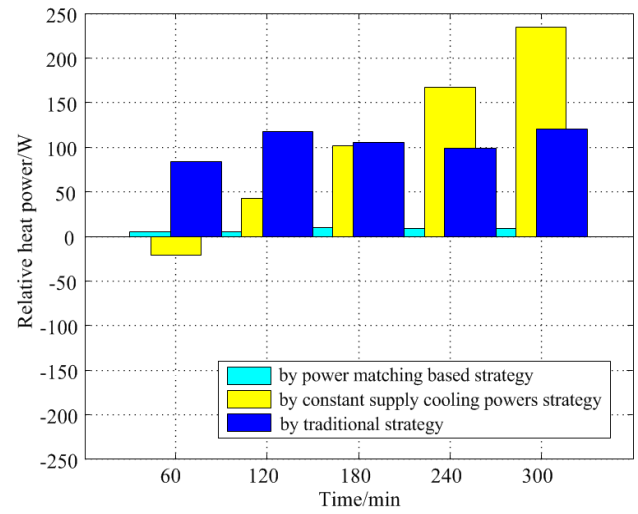
1 structural heat exchange, real-time powers of spindle internal heat dissipations onto heat  
2 sources 1#-3# under 3 different cooling strategies are calculated based on experimental coolant  
3 temperature detections. They are compared with the real-time heat power estimations of  
4 corresponding spindle heat sources, under the progressive spindle rotation speed condition.

5 Fig. 10 (a) illustrates the comparisons of spindle front bearings: 2 existed spindle cooling  
6 strategies can hardly meet the real-time power matching requirement from spindle heat  
7 generations. For the uniform and open-loop strategy, the heat dissipation power of recirculation  
8 coolant has an increasing tendency. Its power values are always lower than the time-variant heat  
9 generation powers and higher than zero. Meanwhile, for the constant supply cooling powers  
10 strategy, the coolant heat dissipation power has an approximately consistent value. In initial  
11 period, the heat dissipation power is slightly higher than heat generation power; but with the  
12 increase of spindle rotation speed, the former is lower than the latter. Unlike existed strategies  
13 above, the power matching based dissipation strategy can guarantee that the real-time heat  
14 dissipation power always approximate to the heat generation power of spindle front bearings,  
15 with the progressive spindle rotation speed.

16 Based on the heat generation-dissipation power comparisons of spindle front bearings in Fig.  
17 10 (a), the real-time power distinctions between the heat generations and dissipations caused by  
18 3 cooling strategies are calculated and compared in Fig. 10 (b). It can be observed that, the  
19 uniform and open-loop strategy have a consistently heating effect for spindle structure; under  
20 the constant supply cooling powers strategy, the spindle structure is slightly cooled by the front  
21 bearings in initial period, but heated subsequently. Specially, under the power matching based  
22 dissipation strategy, the heating effect from front bearings is always near to 0 during the spindle  
23 operation. This clarifies that the power matching based dissipation strategy can realize  
24 effectively the accurate dissipations onto heat generations of spindle front bearings. Actually,  
25 this conclusion can also be obtained by comparisons about the spindle motor and back bearing.  
26 But the related descriptions have been simplified for the length limit of the paper.



(a) Power comparisons between heat generations and dissipations



(b) Relative power comparisons

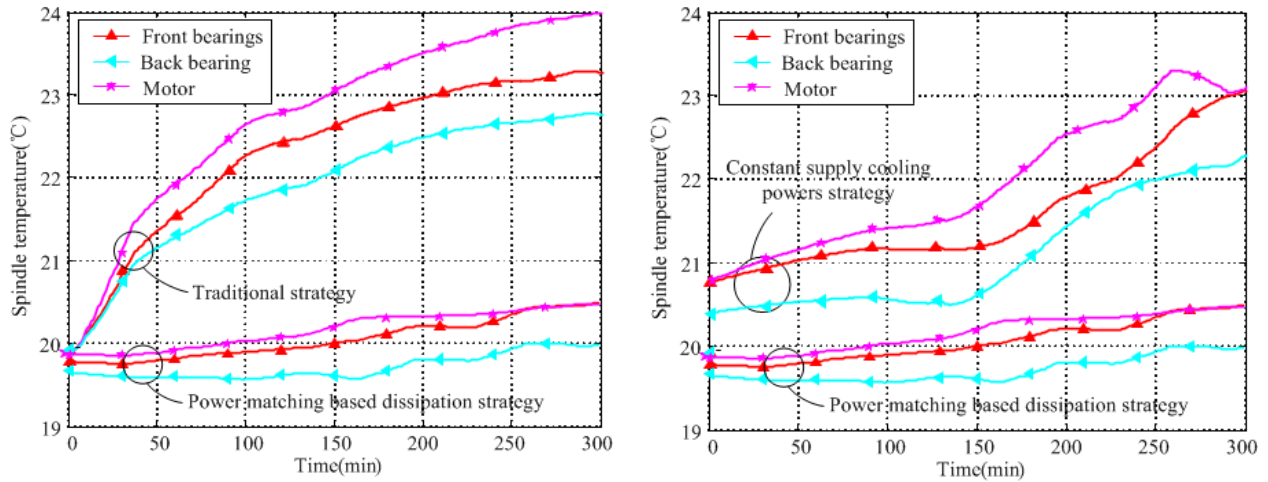
1 Fig. 10 Experimental heat generation-dissipation power analysis about spindle front bearings

## 2 4.3.2 Spindle structural temperatures

3 Based on the RTD sensors in Fig. 9, the experimental temperature values of spindle front  
 4 bearings, motor and back bearing can be obtained by the averaging calculations of real-time  
 5 detections of  $T_A / T_B$ ,  $T_C - T_F$  and  $T_G / T_H$  respectively. Because the motorized spindle unit is  
 6 operating experimentally in a **constant** 20°C workshop, the spindle temperature detections  
 7 nearby heat sources can reflect the behaviors of spindle structural temperatures.

8 In Figs. 11 (a) and (b), the experimental temperatures of spindle front bearings, motor and  
 9 back bearing caused by power matching based dissipation strategy are compared with the ones  
 10 caused by traditional strategy and constant supply cooling powers strategy respectively.  
 11 Obviously, spindle structural temperatures under 2 **existed** strategies have irregular and unstable  
 12 increasing tendencies. The reason is that the power inequality between spindle internal heat  
 13 generations and dissipations can cause the consistently heating effect for spindle structure.  
 14 However, the ones caused by power matching based dissipation strategy are more stable and  
 15 close to ambient temperature (20±0.3°C). This verifies that power matching based dissipation

1 strategy is more accurate and sufficient than the other 2 strategies in dissipations of spindle  
2 internal heat generations.



(a) Compared with traditional uniform,  
open-loop strategy

(b) Compared with constant supply cooling  
powers strategy

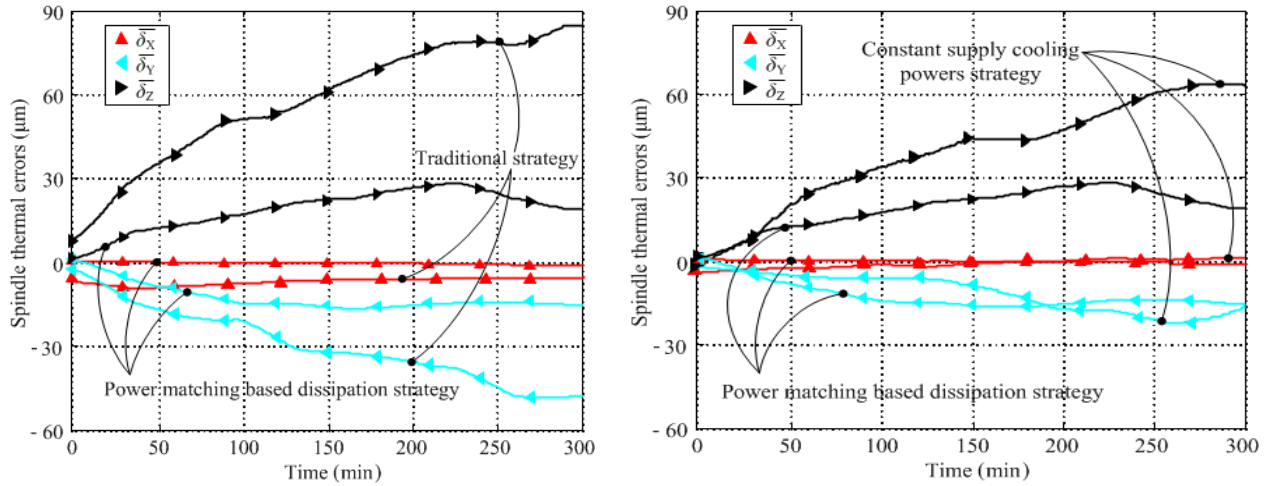
3 Fig. 11 Experiment comparisons of spindle structural temperatures

#### 4 4.3.3 Spindle thermal errors

5 Fig. 9 reveals the geometry relationship between thermal displacements of spindle nose  
6 (Point O) and the detected values from eddy current displacement sensors. This relationship  
7 results in the calculations of experimental linear thermal errors of motorized spindle unit, based  
8 on the detection of the spindle inspection bar.

9 Figs. 12 (a) and (b) illustrate that the spindle linear thermal errors caused by power matching  
10 based dissipation strategy are compared with the ones caused by 2 existed cooling strategies  
11 respectively. It can be observed from Fig. 12 that, spindle thermal errors under 2 existed  
12 strategies are obviously increasing with time, which is always harmful to spindle accuracy and  
13 accuracy stability. This condition is attributed fundamentally to the power inequalities between  
14 spindle internal heat generations and dissipations. Meanwhile, thermal errors caused by power  
15 matching based dissipation strategy are more stable and near to zero than the ones caused by the  
16 other 2 strategies in different degrees. The reducing percentages of steady thermal errors are

1 listed in Table. 1. It can be concluded from the comparisons that the power matching based  
 2 dissipation strategy has the advantage in eliminations of spindle thermal errors. This contributes  
 3 to the improvement of the accuracy and accuracy stability of motorized spindle unit.



(a) Compared with traditional uniform, open-loop strategy

(b) Compared with constant supply cooling powers strategy

Fig. 12 Experiment comparisons of spindle thermal errors

Table 1. Reducing percentages of spindle thermal errors caused by power matching based dissipation strategy

	$\overline{\delta_x}$	$\overline{\delta_y}$	$\overline{\delta_z}$
Compared with traditional uniform, open-loop strategy	94.3%	68.8%	67.4%
Compared with constant supply cooling powers strategy	64.9%	31.7%	54.8%

## 5 Conclusions

This paper mainly introduces a power matching based dissipation strategy for internal heat generations of motorized spindle unit, in order to implement the accurate real-time power matching between spindle heat generations and dissipations. The principle of this strategy is constructed based on the analyses about spindle structural heat generations, dissipations and

1 conduction. Then this strategy can be realized by real-time power estimations of spindle heat  
2 sources and the modified constant supply cooling powers strategy. In summary, conclusions of  
3 this paper are as follows:

4 (1) From the heat transfer perspective, the power inequality between spindle internal heat  
5 generations and dissipations is the fundamental reason for the degradation of the accuracy  
6 and accuracy stability of a motorized spindle unit, which is operating in a constant  
7 temperature (20°C) workshop for precision machining.

8 (2) Compared with existed spindle cooling strategies, the developed power matching based  
9 dissipation strategy has the obvious advantages in the dissipation of spindle internal heat  
10 generations, and it is more effective in spindle structural temperature stabilization and  
11 thermal errors elimination, which has been verified by experiments.

## 12 **Acknowledgment**

13 The authors acknowledge the state S & T projects for upmarket NC machine and  
14 fundamental manufacturing equipment of China (no. 2013ZX04005-013, no.  
15 2014ZX04014-011, no. 2015ZX04005-001, and no. 2016ZX04004-002, resp.).

## 16 **References**

- 17 [1] Weck M, McKeown P, Bonse R, Herbst U. Reduction and compensation of thermal errors  
18 in machine tools. CIRP Annals-Manufacturing Technology 1995; 44: 589-598.
- 19 [2] Timo S, Simon Z, Konrad W. Method for evaluation of energy efficiency of machine tools.  
20 Energy 2015; 93: 1964-1970.
- 21 [3] Chou C, DeBra DB. Liquid temperature control for precision tools. CIRP  
22 Annals-Manufacturing Technology 1990; 39: 535-543.
- 23 [4] Abele E, Altintas Y, Brecher C. Machine tool spindle units. CIRP Annals-Manufacturing  
24 Technology 2010; 59: 781-802.
- 25 [5] Donmez MA, Hahn MH, Soons JA. A novel cooling system to reduce thermally induced  
26 errors of machine tools. CIRP Annals-Manufacturing Technology 2007; 56: 521-524.
- 27 [6] Jedrzejewski J, Kwasny W. Study on reducing energy consumption in manufacturing  
28 systems. Journal of Machine Engineering 2011; 11: 7-20.

- 1 [7] Liu T, Gao, WG, Tian YL, Zhang HJ, Chang WF, Mao K, Zhang DW. A differentiated  
2 multi-loops bath recirculation system for precision machine tools. *Applied Thermal*  
3 *Engineering* 2015; 76c: 54-63.
- 4 [8] Bossmanns B, Tu JF. A thermal model for high speed motorized spindles. *International*  
5 *Journal of Machine Tools and Manufacture* 1999; 39(9):1345–1366.
- 6 [9] Harris TA. *Rolling bearing analysis*, Wiley, New York; 1991.
- 7 [10] Jorgensen BR, Shin YC. Dynamics of machine tool spindle/bearing systems under thermal  
8 growth. *Journal of Tribology* 1997; 119 (4): 875–882.
- 9 [11] De Lacalle NL, Mentxaka AL. *Machine tools for high performance machining*, Springer  
10 *Science & Business Media*; 2008.
- 11 [12] ISO 230-3 2007. Test code for machine tools-Part 3: Determination of thermal actions  
12